HAL
archives-ouvertes.fr

Heterogeneous Clutter Models for Change Detection in PolSAR Imagery

Xuan-Vu Phan, Lionel Bombrun, Gabriel Vasile, Michel Gay

HAL Id: hal-00640858

https://hal.archives-ouvertes.fr/hal-00640858

Submitted on 14 Nov 2011

HETEROGENEOUS CLUTTER MODELS FOR CHANGE DETECTION IN POLSAR IMAGERY

Xuan-Vu Phan, Lionel Bombrun, Gabriel Vasile, and Michel Gay

Grenoble Image Parole Signal et Automatique, GIPSA-lab, Institut National Polytechnique de Grenoble, Grenoble, France

ABSTRACT

The new generation of Synthetic Aperture Radar (RADARSAT-2, TerraSAR-X, ALOS, . . .) allows us to capture Earth surface images with very high resolution. Therefore the possibility to characterize objects has become more and more attainable. Moreover, the short revisit time propertie of these satellites enables the development of techniques of change detection and their applications. Spherically Invariant Random Vector (SIRV) model was designed specifically for the analysis of heterogeneous clutters in high resolution radar images. In this paper, we propose four algorithms of change detection based on different criteria including: Gaussian (sample covariance matrix estimator), Gaussian (fixed point estimator), Fisher texture-based and KummerU-based (Fisher distributed texture).

1. INTRODUCTION

In the past, applications on radar images were largely based on homogeneous clutter models due to the simplicity, easy implementation and fast calculation. However, the recent technology developments of SAR provide very high resolution images. With the new PolSAR sensors, the number of scatters in each resolution cell is remarkably reduced. Therefore the homogeneous hypothesis of the clutter need to be reconsidered.

In this paper, we propose some algorithms of change detection on polarimetric SAR images. The key point consists of combining the SIRV model, which was designed specifically for analysis of heterogeneous clutter, and the stochastic model of Fisher-distributed texture. These new methods provide better estimation of change detection compare to the classic method of Gaussian.

Section II introduces the Gaussian and SIRV models and their application on the change detection aspect. The validation of the algorithms proposed on simulation data will be presented in Section III and in Section IV the case study on PolSAR images of the moutain area located on the border of France, Switzerland and Italy).

2. THE STATISTICAL MODELS: GAUSSIAN AND SIRV

The first step of a change detection algorithm is to recoordinate images taken in different period of time. The next step is to measure the similarity using a statistic model of polarimetric backscatter. The assumption of Gaussianity (homogeneous), typically used in radar imagery, can also be experimented. However, in order to deal with the heterogeneity, new statistical models have been introduced lately.

2.1. Homogeneous Clutter - The Gaussian model

A Gaussian model is a first approach in order to represent the radar clutter. For homogeneous regions, the target scattering vector $\mathbf{k}$ follows a zero-mean circular Gaussian random variable.

The Probability Density Function (PDF) of this process is given by:

$$p_k(\mathbf{k}) = \frac{1}{\pi^p . det[M]} . \exp(-\mathbf{k}^H . [M]^{-1} . \mathbf{k}), \quad (1)$$

where p is the dimension of the target vector k.

This Gaussian process is therefore completely characterized by its covariance matrix $[\mathcal{M}]$.

The Maximum Likelihood estimator of $[M]$, denoted $[\hat{M}_{SCM}]$, is the sample covariance matrix estimator. Its expression is obtained by replacing the statistical average by spatial average:

$$[\hat{M}_{SCM}] = \frac{1}{N} . \sum_{i=1}^{N} \mathbf{k}_i . \mathbf{k}_i^H. \quad (2)$$

The classical Gaussian model provides acceptable results on low-resolution radar images. Most of the applications nowadays use this model for classification [4], change detection [3], etc. However, these applications can only

operate on homogeneous zone or non-textured. Higher resolution radar data requires a more sophisticated model such as the Spherical Invariant Random Vector (SIRV) model.

2.2. The SIRV

Recent PolSAR systems offer very high resolution images and, consequently, much thinner spatial features. This leads to the heterogeneity of the backscattering clutter, which requires higher order of representations than Gaussian model. Therefore, the SIRV model has been considered in order to take into account this heterogeneity.

A SIRV is a compound Gaussian process defined by:

$$\mathbf{k} = \sqrt{\tau}\,\mathbf{z}, \tag{3}$$

where:

- τ is a positive random variable, called *texture*.

- $\mathbf{z}$ is an independent circular complex Gaussian vector with zero mean and covariance matrix $[M] = E\{\mathbf{z}\mathbf{z}^H\}$ (representing the speckle).

For a given covariance matrix $[M]$, the ML estimator of the texture for the pixel i (τ_i) is given by [7]:

$$\hat{\tau}_i = \frac{\mathbf{k}_i^H [M]^{-1}\mathbf{k}_i}{p}, \tag{4}$$

where p is the dimension of the target scattering vector $\mathbf{k}$ ($p = 3$ for the monostatic case).

The ML estimator of the normalized covariance matrix under the deterministic texture case is the solution of the following recursive equation :

$$[\hat{M}]_{FP} = f([\hat{M}]_{FP}) = \frac{p}{N}\sum_{i=1}^{N}\frac{\mathbf{k}_i\mathbf{k}_i^H}{\mathbf{k}_i^H[\hat{M}]_{FP}^{-1}\mathbf{k}_i} \tag{5}$$

with $Tr([\hat{M}]_{FP}) = p$.

Pascal *et al.* have established the existence and the uniqueness, up to a scalar factor, of the Fixed Point estimator of the normalized covariance matrix, as well as the convergence of the recursive algorithm whatever the initialization [7] [8].

By letting $p_\tau(\tau)$ the PDF of the texture random variable τ, the resulting SIRV PDF is given by:

$$p_\mathbf{k}(\mathbf{k}) = \int_0^\infty p_\mathbf{z}(\mathbf{k}|\tau[M])\,p_\tau(\tau)\,d\tau \tag{6}$$

$$= \frac{1}{\pi^p|[M]|}\int_0^{+\infty}\frac{1}{\tau^p}\,\exp\left(-\frac{\mathbf{k}^H[M]^{-1}\mathbf{k}}{\tau}\right)p_\tau(\tau)\,d\tau.$$

3. CHANGE DETECTION ALGORITHMS AND CRITERIAS

3.1. Similarity Measure

Given two populations of two images taken in different period of time (master image and slave image), the similarity measure is defined by:

$$\mathrm{SM} = \mathrm{MLL}_U - \mathrm{MLL}_M - \mathrm{MLL}_S,$$

where MLL_M, MLL_S and MLL_U are the maximum log-likelihood function of the population of Master image, Slave image and the Union of these two respectively. The expression of this function is given by:

$$\mathrm{MLL}_X = \sum_{i\in X}\ln\left(p_\mathbf{k}(\mathbf{k}_i|\theta_X)\right),$$

where θ_X represents the SIRV parameters, and X = U, M or S stands respectively for the union, master and slave images..

3.2. Signal modeling

In the case of Gaussian model, the estimation of the covariance matrix leads directly to the calculation of Maximum Likelihood function. The similarity measure can then be determined without taking into account the distribution of texture. The model is thus more simple and faster. We obtain in this case the test of Box, which was used by Condransen [3] and Morio [5] in change detection and consistency measure. However, when dealing with high resolution images of new generation PolSAR, the extraction and modelisation of texture is crucial due to the heterogeneity of the clutter.

In the SIRV estimation scheme, the covariance matrix is first estimated according to (5). The N texture random variables ($\tau_1, \ldots, \tau_N$) are then derived by (4). The Fisher distribution has been introduced for the modeling of SAR intensity [6]. This distribution has been recently used for the texture modeling of PolSAR images [2], and is well adapted to fit a wide kind of scenes: field, forest, ...

The PDF of a Fisher distribution is defined by:

$$p_\tau(\tau) = \frac{\Gamma(\mathcal{L}+\mathcal{M})}{\Gamma(\mathcal{L})\Gamma(\mathcal{M})} \frac{\mathcal{L}}{\mathcal{M}m} \frac{\left(\frac{\mathcal{L}\tau}{\mathcal{M}m}\right)^{\mathcal{L}-1}}{\left(1+\frac{\mathcal{L}\tau}{\mathcal{M}m}\right)^{\mathcal{L}+\mathcal{M}}}, \quad (7)$$

with $\mathcal{L}, \mathcal{M} \geq 0$, $m > 0$, and $\tau \in \left[0, +\infty\right[$.

The distribution of target vector $\mathbf{k}$ can be written using the KummerU function in the case of Fisher-distributed texture [1]:

$$\begin{aligned}
p_\mathbf{k}(\mathbf{k}) &= \frac{1}{\pi^p|[M]|} \frac{\Gamma(\mathcal{L}+\mathcal{M})}{\Gamma(\mathcal{L})\Gamma(\mathcal{M})} \left(\frac{\mathcal{L}}{\mathcal{M}m}\right)^p \Gamma(p+\mathcal{M}) \quad (8)\\
&\times \quad U\left(p+\mathcal{M}; 1+p-\mathcal{L}; \frac{\mathcal{L}}{\mathcal{M}m}\mathbf{k}^H[M]^{-1}\mathbf{k}\right),
\end{aligned}$$

where U is the confluent hypergeometric function of the second kind.

3.3. Change detection algorithm

In general cases, the change detection algorithm consist of these following steps (Fig 1):

1. Estimation of the covariance matrix of each populations using the Fixed Point algorithm.

2. Extraction of the texture τ using equation (4) (if necessary).

3. Estimation of the parameter(s) θ of the texture distribution p_τ (if necessary).

4. The MLL is calculated using the target vector PDF.

5. The similarity measure (SM) is then computed.

The global scheme of change detection algorithm can be found in Fig 1.

3.4. Criteria

We have implemented four criteria as follow:

- Gaussian: Classic method, entirely depends on the covariance matrix.

- Gaussian Fixed-Point: Gaussian method using the Fixed Point algorithm to estimate the covariance matrix instead of the traditional equation.

- Texture-based: Estimating the statistical parameters of texture extracted while ignoring the covariance matrix.

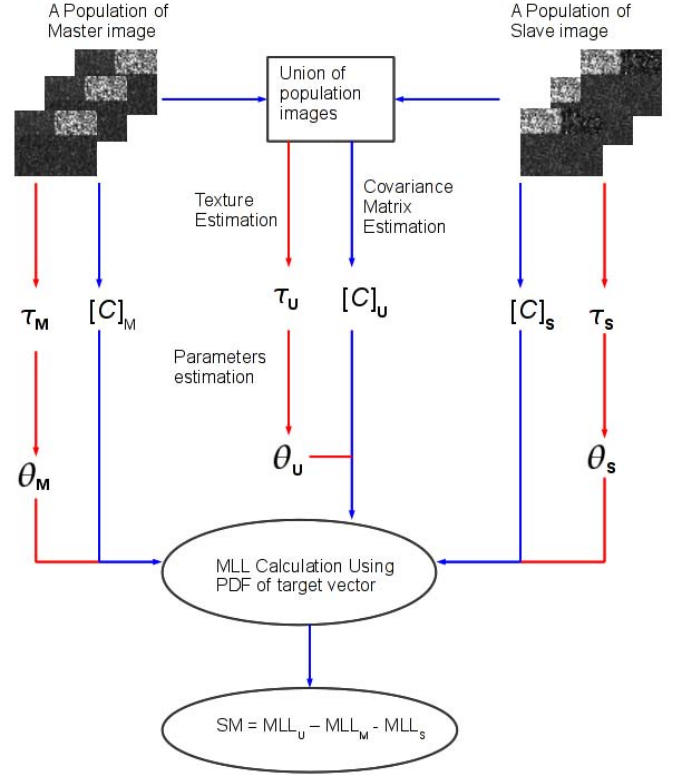- KummerU: The SIRV based on the assumption os Fisher-distributed texture.

Figure 1. The general case of change detection algorithm on a pair of 3-channel polarimetric SAR populations

4. VALIDATION

4.1. Simulated data

4.1.1. Data set introduction

In order to test the performance of the proposed models, a simulated data set has been generated. The data contains two realization of a 3-channel polarimetric SAR images. This data set is composed by 6 different zones. Each zone was created homogeneously or heterogeneously. Moreover, the parameters used to generate the homogeneous (or heterogeneous) distribution are also different. Details can be found in Fig 2 and Table 1.

The model used should output the result showing the areas where there are changes between 2 images and the areas where there is no change. The intensity value of changed area can vary depend on the amount of differences generated. However, the value of unchanged area should be around 0. The theoretical solution of this data set is shown in Fig 3

Table 1. Table of parameters for each zone of data set.

Zone	Image	$p_\tau(\tau)$	m	$\mathcal{L}$	$\mathcal{M}$	[M]	Change ??
Zone 1	Master	Gaussian	n/a	n/a	n/a	M_1	No
	Slave	Gaussian	n/a	n/a	n/a	M_1	
Zone 2	Master	Fisher	1.5	2	3	M_2	No
	Slave	Fisher	1.5	2	3	M_2	
Zone 3	Master	Fisher	1	1.5	2.5	M_3	Yes
	Slave	Fisher	1.7	2.1	3.1	M_5	
Zone 4	Master	Gaussian	n/a	n/a	n/a	M_4	Yes
	Slave	Fisher	1.7	2.1	3.1	M_5	
Zone 5	Master	Fisher	1.7	2.1	3.1	M_5	Yes
	Slave	Fisher	1.1	2.9	3.9	M_4	
Zone 6	Master	Fisher	1.7	2.1	3.1	M_5	Yes
	Slave	Gaussian	n/a	n/a	n/a	M_3	
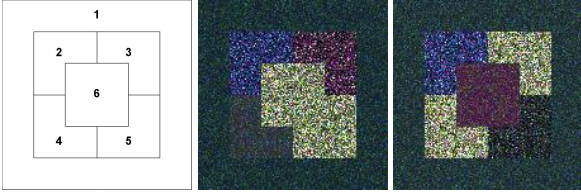
Figure 2. The RGB images of 2 generated polarimetry images, where 3 channels $\mathbf{k}_1, \mathbf{k}_2, \mathbf{k}_3$ of polarimetry correspond to 3 channels of color R G B. Left image: Zones of the generated data, center image: Master, right image: Slave

4.1.2. Gaussian model (Homogeneous)

The change detection algorithm using Gaussian model was tested on different sizes of sliding window: $7 \times 7, 11 \times 11$ and 15×15 (Fig 4).

The size of sliding window plays an important role on the quality of the output result. If the size of sliding window is small, the border effect is reduced, however the amount of noise will increase. Meanwhile a bigger size of sliding window gives a more solid result with blur effect, at the cost of increasing border effect.

Notice that while both background and upper left zone are unchanged, the upper left zone doesn't appear as clearly as the background, this is due to the ineffectiveness of Gaussian model while using on heterogeneous clutter.

4.1.3. KummerU model (SIRV)

The KummerU model shows a result with higher quality than the previous classic model (Fig 5). The output images are more solid and the border effect is remarkably reduced.

Table 2 shows the mean values and standard deviation (std) of zone 1 and zone 2 of Gaussian and KummerU results. The zone 1 was generated with a Gaussian-distributed texture, therefore both models output a re-
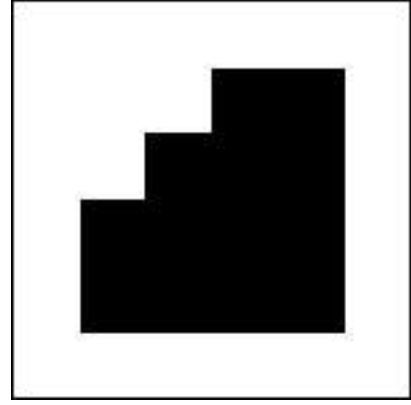

Figure 3. The theoretical result of change detection on the generated data set
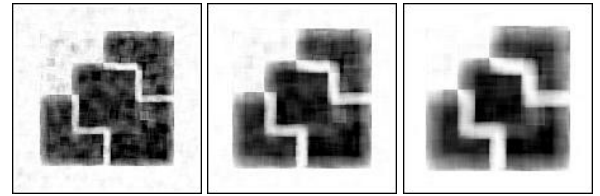

Figure 4. The result of change detection using Gaussian model. From left to right, the sizes of sliding window are respectively $7 \times 7, 11 \times 11, 15 \times 15$

sult with the mean values near zero (≈ 4.5) and low std (smooth result). Meanwhile, the result of Gaussian model on zone 2 has a higher mean (14.02) compare to the KummerU model (5.06).

4.1.4. Result Evaluation

Before the conclusion on these 2 methods, it is also interesting to evaluate the result through quantifying. We now define 2 magnitude values:

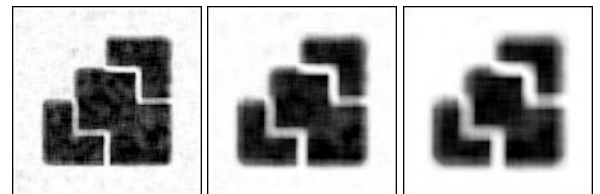- The probability of detection (note p_d): the probability of detecting a change that is correct

Figure 5. The result of change detection using KummerU model. From left to right, the sizes of sliding window are respectively $7 \times 7, 11 \times 11, 15 \times 15$

Table 2. Comparison of Gaussian and KummerU results on zone 1 and zone 2 (without taking the border effect).

	Zone 1		Zone 2	
	mean	std	mean	std
Gaussian	5.02	0.78	14.02	2.26
KummerU	4.28	0.91	5.06	0.75

- The probability of false alarm (note p_{fa}): the probability of detecting a change while there is in fact no change.

Let A the area of surface where there are real changes (ground truth), and B the area of change deduce from the result of algorithm. We then define the probability of detection (p_d) and probability of false alarm(p_{fa}) through the following formulas:

$$p_d = \frac{N_{A \cap B}}{N_A} \tag{9}$$

$$p_{fa} = \frac{N_{\bar{A} \cap B}}{N_{\bar{A}}} = \frac{N_B - N_{A \cap B}}{N_{\bar{A}}}, \tag{10}$$

with N_X the number of pixels in the area X.

These equations satisfy the conditions $p_d < 1$ and $p_{fa} < 1$. Note that if the algorithm detects the whole map as changed, then both p_d and p_{fa} will receive the value 1. We can now plot the ROC (Receiver Operating Characteristic) curve (Fig. 6).
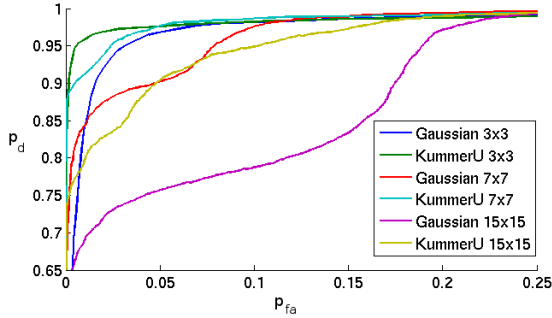

Figure 6. Plotting the ROC curve for different sizes of sliding window

Table 3. Values of p_d sorted in ascending order with the given $p_{fa} = 0.05$

	Gaussian 15×15	Gaussian 11×11	Gaussian 7×7	KummerU 15×15	KummerU 11×11	KummerU 7×7
p_d	0.7578	0.8293	0.9036	0.9049	0.9446	0.9774

Table 3 shows the values of p_d of each curves with the given value of $p_{fa} = 0.05$ sorted in ascending order.

As we can see, again the size of sliding window has a big influence on the quality of result. Also the heterogeneous model KummerU has been proven to be more effective than the Gaussian model. However, the advantage of Gaussian model lies in its performance. Some tests have been conducted and the results show that on a same dataset, an application using Gaussian model is approximately 50-60 times faster than the KummerU model. This is due to the high complexity of calculation. So the choice of algorithm has to be compromised between the quality of result and the performance of the application.

4.2. Multivariate Change Detection on Simulated data

4.2.1. Data set introduction

This test has been carried out to show the different algorithms applying on a heterogenous simulated data set. Same as the first test, this data set consists of a pair of PolSAR images: Master and Slave, each image is divided into six zones. Every zone is generated heterogeneously, with parameters according to Table 4. A visualizable version of the data set is shown in Fig 7 while the expecting result can be found in Fig 8.

Table 4. Table of parameters for each zone of data set.

Zone	Image	m	$\mathcal{L}$	$\mathcal{M}$	[M]	Parameter Changes
Zone 1	Master	3	1	2	M_1	No Change
	Slave	3	1	2	M_1	
Zone 2	Master	1.5	2	3	M_2	$\mathcal{L}$ and $\mathcal{M}$
	Slave	1.5	6	7	M_2	
Zone 3	Master	1	1.5	2.5	M_3	[M]
	Slave	1	1.5	2.5	not M_3	
Zone 4	Master	0.5	2.5	3.5	M_4	No Change
	Slave	0.5	2.5	3.5	M_4	
Zone 5	Master	1.7	2.1	3.1	M_5	No Change
	Slave	1.7	2.1	3.1	M_5	
Zone 6	Master	1.1	2.9	3.9	M_5	m
	Slave	4.1	2.9	3.9	M_3	
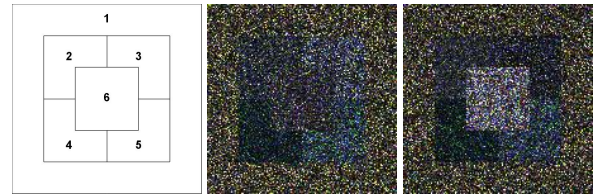
Figure 7. The RGB images of 2 generated polarimetry images, where 3 channels $\mathbf{k}_1, \mathbf{k}_2, \mathbf{k}_3$ of polarimetry correspond to 3 channels of color R G B. Left Image: Map of zones, Center image: Master, right image: Slave

In this data set, there are three types of changes, each type concerns different parameters of distribution: the scale parameter (m), the shape parameters ($\mathcal{L}$ and/or $\mathcal{M}$), the covariance matrix ([$\mathcal{C}$]). The algorithms proposed

are expected to show their diversity in detecting types of changes.
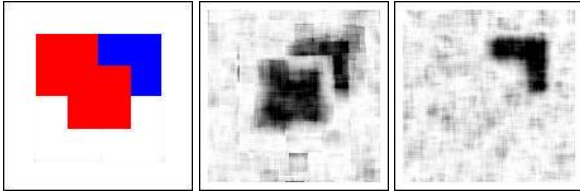
4.2.2. Result Evaluation

Figure 8. The theoretical result (left) with changes in texture distribution paramaters cover (red zone) and changes in covariance matrices (blue zone) , the result of change detection using algorithm Gaussian (center) and Fixed Point Gaussian (right)
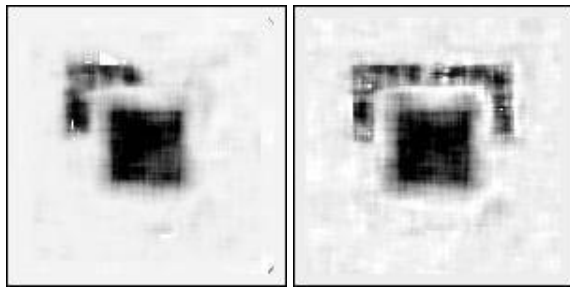

Figure 9. The result of change detection using algorithm Fisher texture-based (left) and KummerU-based (right)

The result obtained using Gaussian and Fixed Point Gaussian algorithms can be found in Fig 8 while Fig 9 shows the result of Fisher texture-based and KummerU-based algorithms. The Gaussian and Fixed Point Gaussian algorithms are capable of detect the changes in the covariance matrices (zone 3), however they cannot detect the changes in the parameters of Fisher distribution ($\mathcal{L}$, $\mathcal{M}$). This is due to the characteristic of Gaussian model which measure the similarity based on mean values and covariance matrix. As expected, the result of Fixed Point Gaussian algorithm appears to be smoother than the classical Gaussian's because of the more appropriate method in estimation of covariance matrix.

The changes in texture mean, $\mathcal{L}$, $\mathcal{M}$ and m are detected using Fisher texture-based algorithm (zone 2 and 6). Nevertheless, it was unable to detect the changes in covariance matrix (zone 3). This algorithm is based on texture modeling (the τ part of SIRV model) while completely ignoring the Gaussian part (the $\mathbf{z}$ part of equation 3). Meanwhile, the KummerU-based algorithm, which is based on the SIRV model applying specifically on Fisher-distributed texture, shows a better result in detecting all types of changes.

5. CASE STUDY: TERRASAR-X

Some tests have been conducted on the real PolSAR images of the mountain zone of Taconnaz (border of France, Switzerland and Italy). The change detection algorithm was used on two set of dual-Pol TerraSAR-X images (HH and VV) of size 4406×3729 pixels which were taken on the same area in 17 January 2009 and 28 January 2009 respectively. Images are provided by the German Aerospace Agency (DLR) through the project "Monitoring Temperate Glacier Activity by X-band Polarimetric SAR Interferometry". Due to the huge size of image, we have select two zones of which changes are the most visualizable. The results can be found in Fig 10 and Fig 11. At this time we do not know if this change detection is the movement of the Taconnaz glacier or the evolution of the snowpack. Additional informations are needed. The method of tracking texture to obtain the velocities of the Astrolabe glacier in Antarctica that we developed and validated and in-situ measurements should allow us to remove this uncertainty. These are the future work.
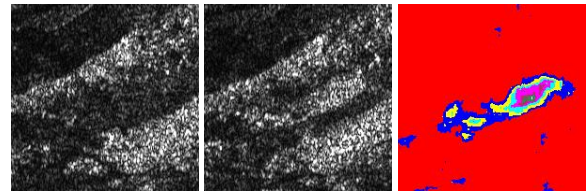

Figure 10. The result of change detection on dual-Pol TerraSAR-X images. Left: Master image, center: Slave image, right: Result of change detection
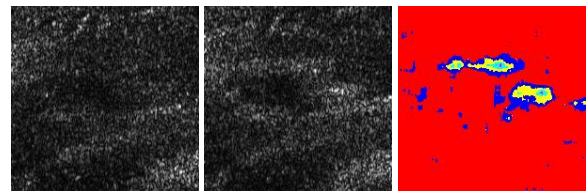

Figure 11. The result of change detection on dual-Pol TerraSAR-X images. Left: Master image, center: Slave image, right: Result of change detection

6. CONCLUSION

In this paper, we have proposed a change detection algorithm based on texture modeling in PolSAR images. The existed algorithm based on the assumption of Gaussianity works well on low-resolution SAR images but does not provide a good result in the cases of new generation SAR images with very high resolution. In this context, the assumption of homogeneity cannot be assured, therefore, new model has been introduced in order to take into account the heterogeneous clutter. The proposed algorithm, KummerU, which is based on SIRV model, has

been passed through a validation on both simulated and real TSX images on glaciers and has shown its capability of change detection on high resolution PolSAR images. The results are generally better than the classical methods.

ACKNOWLEDGMENT

REFERENCES

[1] L. Bombrun and J.-M. Beaulieu. Fisher Distribution for Texture Modeling of Polarimetric SAR Data. *IEEE Geoscience and Remote Sensing Letters*, 5(3), July 2008.

[2] L. Bombrun, G. Vasile, M. Gay, and F. Totir. Hierarchical Segmentation of Polarimetric SAR Images using Heterogeneous Clutter Models. *IEEE Transactions on Geoscience and Remote Sensing*, 2010, to appear.

[3] K. Conradsen, A. A. Nielsen, J. Schou, and H. Skriver. A Test Statistic in the Complex Wishart Distribution and its Application to Change Detection in Polarimetric SAR Data. *IEEE Transactions on Geoscience and Remote Sensing*, 41(1), 2003.

[4] J.S. Lee, M.R. Grunes, T.L. Ainsworth, L.J. Du, D.L. Schuler, and S.R. Cloude. Unsupervised Classification Using Polarimetric Decomposition and the Complex Wishart Classifier. *IEEE Transactions on Geoscience and Remote Sensing*, 37(5):2249–2258, 1999.

[5] J. Morio, P. Réfrégier, F. Goudail, P. C. Dubois-Fernandez, and X. Dupuis. Information Theory-Based Approach for Contrast Analysis in Polarimetric and/or Interferometric SAR Images. *IEEE Transactions on Geoscience and Remote Sensing*, 46(8), 2008.

[6] J-M. Nicolas. Application de la Transformée de Mellin: Étude des Lois Statistiques de l'Imagerie Cohérente. In *Rapport de recherche, 2006D010*, 2006.

[7] F. Pascal, Y. Chitour, J. P. Ovarlez, P. Forster, and P. Larzabal. Covariance Structure Maximum-Likelihood Estimates in Compound Gaussian Noise : Existence and Algorithm Analysis. *IEEE Transactions on Signal Processing*, 56(1):34–48, 2008.

[8] F. Pascal, P. Forster, J. P. Ovarlez, and P. Larzabal. Performance Analysis of Covariance Matrix Estimates in Impulsive Noise. *IEEE Transactions on Signal Processing*, 56(6):2206–2216, 2008.